EFFECT OF LATERAL WALLS ON THE PROPAGATION CHARACTERISTICS OF FINITE-WIDTH CONDUCTOR-BACKED COPLANAR WAVEGUIDES

C.-C. Tien, C.-K. C. Tzuang and J. Monroe

Indexing terms: Microwave device, Circuit theory and design

The connection of the side planes of finite-width conductor-backed coplanar waveguide (FW-CBCPW) to the ground through lateral walls suppresses the undesired microstrip-like (MSL) mode and provides a wide frequency range over which singlemode propagation occurs. The leakage or resonance phenomena of the higher-order modes can be avoided, if the distance separating the lateral walls is carefully designed.

Introduction: CBCPW circuits are attractive structures for hybrid and monolithic microwave integrated circuits (MICs/MMICs) as two coplanar side planes ease the implementation of the shunt element and the integration of active devices. The additional backside conductor, however, may cause parallel-plate-mode leakage [1] when the side planes are infinitely wide. This implies that the energy coupling between adjacent lines is inevitable. If the side-plane width is finite, the CBCPW supports a zero-cutoff MSL mode. Mode conversion between MSL and CPW modes [2] occurs at discontinuities and may even cause the MSL mode to resonate in the FW-CBCPW through-line when two ends of each side plane are shorted to the backside plane [3]. Such effects severely deteriorate the FW-CBCPW circuit performance and should be avoided in circuit design.

Fig. 1 shows the cross-sectional geometry of a modified FW-CBCPW. It is postulated that suppression of the zero-cutoff MSL mode can be achieved by longitudinally connecting the FW-CBCPW side planes to the backside plane. The lateral walls that provide the connection are shown in Fig. 1.

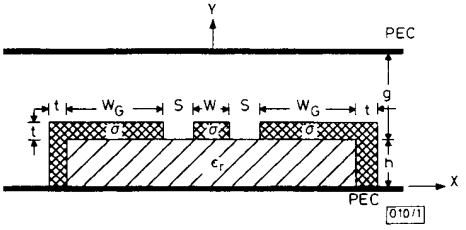

Fig. 1 *Cross-sectional geometry of the modified FW-CBCPW with the lateral side-plane edges shorted to the lower ground plane*

Structural parameters are as follows: $W = S = 0{\cdot}508$ mm, $h = 0{\cdot}2g = 0{\cdot}635$ mm, $t = 17\,\mu$m, $\sigma = 5{\cdot}8 \times 10^7$ S/m (copper), and $\varepsilon_r = 10{\cdot}2$; two cases of W_G, say 1·0 and 0·5 mm, are studied

In this Letter, the full-wave mode-matching method [3, 4] is applied to analyse the propagation characteristics of this waveguiding structure. After the theoretical analysis, the multimode effect is verified experimentally by measuring the transmission characteristics of the modified FW-CBCPW through-line.

Lateral-wall effect: Fig. 2 shows the dispersion characteristics obtained from the full-wave analysis of the FW-CBCPW structure for $W_G = 1{\cdot}0$ and 0·5 mm. It can be clearly seen that our approach to grounding the side planes successfully causes single CPW mode propagation below a critical frequency. The singlemode frequency range increases from 17 to 26 GHz as the side-plane width is decreased from 1 to 0·5 mm. Above this critical frequency, the leaky or bounded first higher-order mode starts propagating. In the region in which the higher-order mode propagates with normalised phase and leaky (attenuation) constants both less than unity, an appreciable leakage effect is observed. For $W_G = 1{\cdot}0$ and 0·5 mm, the above-mentioned leaky regions as shown in Fig. 2 are 17–19 GHz and 26–30·5 GHz, respectively. When a top cover is placed above the FW-CBCPW, as shown in Fig. 1, the leakage energy spreads out of the slot regions in the form of parallel-cover modes. If the top cover is removed, the leaky mode radiates power into space at an angle to the transmission line. The leaky higher-order mode is cutoff (evanescent)

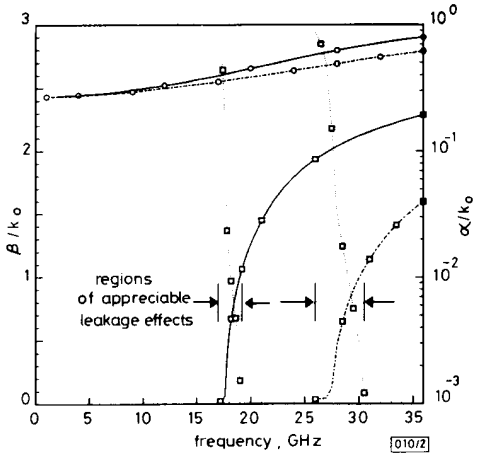

Fig. 2 *Dispersion characteristics of modified FW-CBCPW as shown in Fig. 1*

Normalised phase constants for $W_G = 1{\cdot}0$ mm:
—○— CPW mode
—□— First higher-order mode
For $W_G = 0{\cdot}5$ mm:
- -○- - CPW mode
- -□- - First higher-order mode
····· Normalised leaky (attenuation) constants of first higher-order mode

when its normalised leakage (attenuation) constant becomes larger than unity. Below the appreciable leakage region, discontinuities in an FW-CBCPW circuit cannot convert the CPW mode to the leaky higher-order mode and thus no power leakage can occur. Above this region, the higher-order mode becomes bounded and the significant mode conversion and resonance of higher-order modes are expected in the modified FW-CBCPW circuits.

Experimental verification: The transmission characteristics of the modified FW-CBCPW through-line with $W_G = 1{\cdot}0$ mm were measured using an HP 8510 network analyser. The obtained scattering parameters are presented in Fig. 3. The plot verifies the initial postulation that from DC to 17 GHz

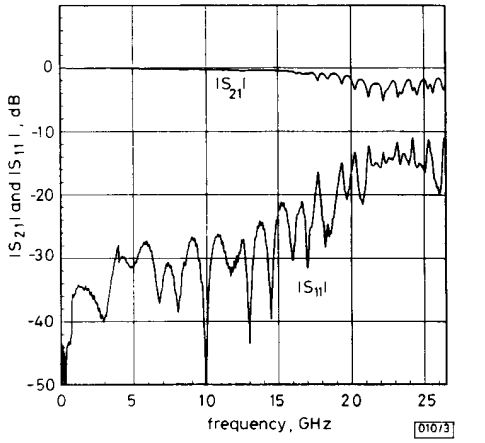

Fig. 3 *Measured transmission ($|S_{21}|$) and reflection ($|S_{11}|$) characteristics of modified FW-CBCPW through-line of Fig. 1*

Side-plane width $W_G = 1{\cdot}0$ mm; through-line length $L = 38{\cdot}1$ mm

the addition of lateral grounding walls prevents the propagation and the resonance of the MSL mode in the FW-CBCPW through-line [3]. The first two frequencies of resonance of the first higher-order mode at 17·7 and 18·4 GHz, as shown in Fig. 3, are in the region of appreciable leakage effect. Between 18 and 19 GHz, the reflected energy of the first higher-order mode that has been converted from the CPW mode at the port discontinuities strongly leaks out of the through-line. This is verified by the observed decrease in the magnitude of the reflection coefficient ($|S_{11}|$). Above 19 GHz, the theoretical results show that the higher-order mode becomes bounded ($\beta/ko > 1$). Its phase constant increases rapidly towards the value of that of a CPW mode. Consequently, the mode-coupling effect occurs between two nodes that results in the significant higher-order-mode resonance phenomena in the higher frequency range as shown in Fig. 3. The structural parameters of the FW-CBCPW are designed to obtain the 50 Ω characteristic impedance of the CPW mode in the low frequency limit. Above 23 GHz, a 20% increase of CPW-mode characteristic impedance is observed from the full-wave analysis. Such impedance mismatch between the 50 Ω probe and the FW-CBCPW causes the resonance of the dominant CPW mode, such as the resonance peaks at 23·5, 24·5 and 25·6 GHz observed in Fig. 3.

Conclusion: The CBCPW has been modified by connecting its side planes to the backside metal with lateral walls. Both theoretical and measured results show that by means of careful design the propagation and resonance of the zero-cutoff MSL mode can be suppressed. Above a certain frequency limit, the first higher-order mode leaks in the form of a parallel-cover mode. When the frequency is further increased, this mode becomes bounded and resonant in the FW-CBCPW through-line at higher discrete frequencies. It has been shown that decreasing the width of the side planes may lead to an increase in the cutoff frequency of the first higher-order mode and thus broaden the useful frequency range of the FW-CBCPW.

Acknowledgment: This work was supported in part by the National Science Council and the Chung-Shan Institute of Science & Technology, Republic of China, under Grant NSC81-040-E009-120 and Contract CS-82-0210-D006-026.

11th May 1993

C.-C. Tien and C.-K. C. Tzuang (*Institute of Communication Engineering, National Chiao Tung University, No. 1001, Ta Hsueh Road, Hsinchu, Taiwan, Republic of China*)

J. Monroe (*Electrical and Electronic Systems Engineering, School of Queensland University of Technology, GPO Box 2434, Brisbane, QLD 4001, Australia*)

References

1 SHIGESAWA, H., TSUJI, M., and OLINER, A. A.: 'Conductor-backed slot line and coplanar waveguide: Dangers and full-wave analyses'. IEEE MTT-S Int. Microwave Symp. Dig., 1988, pp. 199–202

2 JACKSON, R. W.: 'Mode conversion at discontinuities in finite-width conductor-backed coplanar waveguide', *IEEE Trans.*, 1989, **MTT-37**, pp. 1582–1589

3 TIEN, C.-C., TZUANG, C.-K. C., PENG, S. T., and CHANG, C.-C.: 'Transmission characteristics of finite-width conductor-backed coplanar waveguide'. To be published in IEEE MTT-T Special Issue on Modeling and Design of CMMICs, Sept. 1993

4 TZUANG, C.-K. C., CHEN, C.-D., and PENG, S. T.: 'Full-wave analysis of lossy quasi-planar transmission line incorporating the metal modes', *IEEE Trans.*, 1990, **MTT-38**, pp. 1792–1799

NEW EXPERIMENTAL TECHNIQUE FOR FAST AND ACCURATE MOSFET THRESHOLD EXTRACTION

F. Corsi, C. Marzocca and G. V. Portacci

Indexing terms: MOSFETs, Semiconductor device testing

Threshold voltage extraction for MOS devices is translated into the easier task of locating a minimum in a derived function of I_{DS} and V_{GS}. The technique, which provided excellent results on both simulated (SPICE) and experimental data, has been tested on several MOSFETs from different processes and has been implemented into an automated tool instead of more costly optimisation based techniques.

Introduction: It has been observed [1] that, although a large number of parameters are needed to accurately model MOSFET behaviour at circuit level, the most frequently encountered process fluctuations influence the values of essentially three parameters: the zero bias threshold voltage V_{TO}, the transconductance parameter K_P, and the mobility degradation factor θ. Most extraction procedures start with the evaluation of the bias dependent threshold voltage V_{th}. The importance of accurate threshold extractions is apparent because these values may adversely affect the next extracted parameters. We developed an original technique for a precise evaluation of V_{th} which is fast enough to be employed for statistical analysis [2, 3] and needs no careful choice of I_{DS} against V_{GS} points of the transcharacteristic [1].

Outline of extraction technique: We define a family of curves where Beta is plotted against gate bias V_{GS} for various values at a constant V_p, as shown in Fig. 1. The Beta function is

$$\text{Beta}(V_{GS}, V_P) = \frac{I_{DS}}{V_{GS} - V_p} \quad (1)$$

where $V_{GS} > V_p$ and various values of V_p are chosen in the region of the expected threshold voltage.

These functions have the property that if V_p is equal to $V_m = V_{th} + (\alpha/2) \times V_{DS}$ (α is a constant parameter which is related primarily to small channel effects, the body effect, and

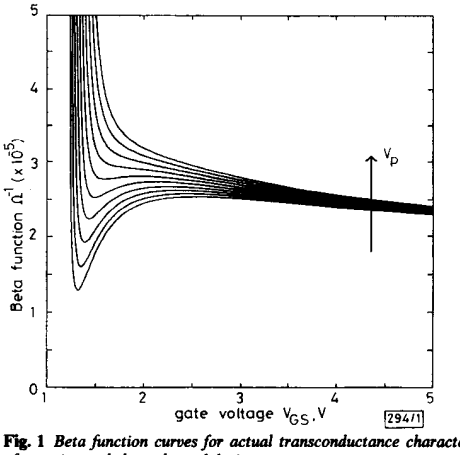

Fig. 1 *Beta function curves for actual transconductance characteristics of experimental short channel device*

the surface inversion potential), they represent a first order approximation (apart from the scaling factor V_{DS}) to the gain parameter β in the linear region of operation. The effects of the drain and source parasitic resistance R_s and R_d are negligible due to the very low value of the product $(R_s + R_d) \times I_{DS}$ ($\simeq 10^{-5}$ V) when the gate voltage is close to V_{th}, compared to V_{DS} which is usually in the range 0·01–0·1 V. At the onset of weak surface inversion, the value of Beta sharply deviates from β, and eqn. 1 no longer has any physical meaning because the I_{DS} current exhibits a quadratic dependence on V_{GS}. Thus Beta acts as powerful indicator of the onset of subthreshold I_{DS} against V_{GS} characteristics.

For $V_p > V_m$, the Beta functions are monotonically decreasing against V_{GS} and for $V_p \leqslant V_m$ the Beta functions exhibit a relative minimum, as shown in Fig. 1.